

# Resource Allocation for Periodic Traffic in Wireless Sensor Network

Aoto Kaburaki<sup>1</sup>, Koichi Adachi<sup>1</sup>, Osamu Takyu<sup>2</sup>, Mai Ohta<sup>3</sup>, Takeo Fujii<sup>1</sup>

<sup>1</sup>Advanced Wireless & Communication research Center (AWCC), The University of Electro-Communications, Tokyo, Japan,

<sup>2</sup>Shinshu University, Nagano, Japan, <sup>3</sup>Fukuoka University, Fukuoka, Japan

**Abstract**—With the fast growth of Internet-of-things (IoT) and machine-to-machine (M2M) communications technology, low-power wide area networks (LPWAN) such as long-range wide area network (LoRaWAN) are attracting attention. One of the main applications of LPWAN is information collected from a large number of sensor nodes, where network traffic is generally dominated by periodic uplink (UL) traffic. In LPWAN, each sensor node transmits packets at arbitrary timing, which causes packet collisions and degrades the system communication quality. Especially in the case of periodic UL, continuous packet collisions may occur. Therefore, this paper proposes a centralized radio resource allocation scheme that avoids packet collisions of periodic traffic in LPWANs, taking into account the characteristics of the periodical traffic. The computer simulation results show that the proposed scheme can improve the average packet delivery ratio (PDR) by 18% and the age-of-information (AoI) performance compared to the ALOHA protocol.

**Index Terms**—Wireless sensor networks, LPWA, LoRaWAN, Resource allocation, Periodic traffic

## I. INTRODUCTION

The Internet-of-Things (IoT) has made remarkable progress in the past few years. In IoT, various devices are equipped with functions to connect to the Internet and machine-to-machine (M2M) communication technologies. Especially wireless sensor networks (WSN) have become increasingly popular in various applications due to miniaturized wireless devices with lower energy consumption [1]. WSN aims to collect environmental information such as temperature and CO<sub>2</sub> using sensors equipped with wireless communication functions. In industrial applications, such as smart cities and smart agriculture, low power wide area networks (LPWAN) are attracting attention for their capability to realize a wide communication area of several kilometers at a low cost [2]. Generally speaking, wireless sensor nodes in a particular area monitor the surrounding environment and periodically transmit the sensing data to an information aggregation station, such as a gateway (GW). Thus, the LPWAN traffic is dominated by periodic uplink (UL) traffic.

LPWAN typically adopts an asynchronous random access protocol such as pure ALOHA for the medium access control (MAC) layer. In pure ALOHA, each sensor node transmits packets immediately after generating a packet. Thus, multiple sensor nodes may simultaneously transmit packets on the same wireless resource, which causes packet collision at a receiving device. Thus, a carrier sense (CS) based random access protocol has been introduced in LPWAN to reduce packet collisions [3]. The CS enables autonomous decentralized packet colli-

sion avoidance without synchronization between sensor nodes. However, since sensor nodes are distributed over a wide area in LPWAN, CS may not work properly, and packet collision avoidance becomes difficult [4]. As described above, packet collisions occur in LPWANs due to the simple MAC layer access protocol and its wide communication area. The packet reception failure happens more frequently as the number of sensor nodes increases in the system due to increased packet collision probability. Furthermore, in an LPWAN with periodic traffic, some combinations of packet generation cycles cause repetitive packet collisions for specific nodes [5].

Given such a background, this paper proposes a centralized radio resource allocation scheme for LPWAN with periodic traffic. The purpose is to avoid repetitive packet collisions in an LPWAN with a large number of nodes and periodical traffic. For information periodically collected from multiple sensor nodes, not only improving the packet delivery rate (PDR) but also keeping the received data fresh at the GW is essential. For evaluation of information freshness, age-of-information (AoI) has been considered as an appropriate metric [6]–[8]. Improving the PDR through simple ways, e.g., random backoff, may degrade the AoI. Thus, we aim to improve the PDR while balancing the AoI degradation. The GW allocates an appropriate frequency channel and transmission timing offset to each node. The joint allocation of a frequency channel and transmission timing offset is a combinatorial optimization. Thus, it is challenging to solve it due to combinatorial explosion as the number of nodes increases. Thus, we tackle this problem by using a sequential resource allocation algorithm based on packet collision prediction for each node. The numerical evaluation shows that the proposed scheme improves PDR performance by about 18% compared to conventional LPWAN systems.

The remainder of this paper is organized as follows. Section II describes the LoRaWAN-based system model. The proposed resource allocation scheme based on periodic traffic characteristics is presented in Sect. III. Section IV provides computer simulation results. Section V concludes the paper.

## II. SYSTEM MODEL

This paper considers a network consisting of  $I$  LoRaWAN nodes ( $\mathcal{I} = \{1, \dots, i, \dots, I\}$ ) and one GW. Nodes are randomly and uniformly distributed in a circular communication area of radius  $r$  [m] centered on the GW, as shown in Fig. 1. A node selects one of  $K$  orthogonal frequency channels

( $\mathcal{K} = \{1, \dots, k, \dots, K\}$ ) to transmit data packets. The nodes and GW operate in a half-duplex communication mode.

#### A. Nodes and GW

1) *Nodes*: This paper assumes all the nodes operate in Class A, which is the mandatory feature in a LoRaWAN system. We assume periodic UL traffic, which happens in environmental monitoring and other applications [9], [10]. Node  $i$  generates a UL data packet of  $B_{\text{data}}$  [bit] at every UL packet generation cycle  $G_{p,i}$  [min].  $G_{p,i}$  is randomly and uniformly selected from the integer values in the range  $[1, G_p^{\text{max}}]$  with  $G_p^{\text{max}}$  being the maximum UL packet generation cycle. The first packet generation time of node  $i$ ,  $T_i^{\text{FP}}$ , is randomly selected from the range  $[0, G_{p,i}]$ . Node  $i$  transmits the generated UL packet as an unconfirmed packet to the GW using frequency channel  $k_i \in \mathcal{K}$  and spreading factor (SF)  $S_i \in \mathcal{S}$ , where  $\mathcal{S}$  is a set of available SFs. Node  $i$  selects  $S_i$  based on the received signal-to-noise power ratio (SNR) at the GW [11]. In some countries, including Japan, a node must follow the duty cycle (DC) constraint defined by the law. Since the UL packet generation cycle is much larger relative to the DC constraints, the UL traffic from each node always satisfies the DC constraint.

2) *GW*: Upon reception of a UL packet from node  $i$ , the GW shall transmit DL packets while node  $i$  opens a receiving window. The GW transmits the DL packet to node  $i$  using the same SF  $S_i$ , same frequency channel  $k_i$ . The DL packet transmission duration is denoted by  $T_{L,i}$  [sec]. Since the GW generates and tries to transmit DL packets to multiple nodes, it may not satisfy the DC constraint as the number of nodes increases. Thus, once the GW transmits a DL packet on a frequency channel, it stops DL packet generation on the frequency channel. The waiting time,  $T_{k_i}^{\text{DC}}$ , required to satisfy the DC after transmitting a DL packet to node  $i$  is given as

$$T_{k_i}^{\text{DC}} = \left( \frac{1 - D_c}{D_c} \right) T_{L,i} \quad (1)$$

where  $D_c \in (0, 1]$  is the DC.

#### B. Packet Reception Model

The received SNR,  $\gamma_{\text{SNR},i}$  [dB], and signal-to-interference power ratio (SIR),  $\gamma_{\text{SIR},i}$  [dB], of node  $i$  at the GW are given by

$$\begin{cases} \gamma_{\text{SNR},i} &= P_{r,i} - (N_0 + 10 \log_{10} W + NF) \\ \gamma_{\text{SIR},i} &= P_{r,i} - \sum_{i' \in \mathcal{I}_i} P_{r,i'} \end{cases}, \quad (2)$$

where  $P_{r,i}$  is the received signal power of node  $i$  at the GW,  $N_0$  [dBm/Hz] is the noise power spectrum density,  $NF$  [dB] is the noise figure, and  $\mathcal{I}_i$  is the set of interfering nodes in the system simultaneously transmitting a data packet in the same frequency channel as node  $i$ . If  $\gamma_{\text{SNR},i}$  and  $\gamma_{\text{SIR},i}$  exceed the SNR and SIR thresholds, shown in Table I, the GW succeeds in receiving the UL packet from node  $i$ .

### III. PROPOSED SCHEME

In the proposed centralized resource allocation scheme, the GW allocates frequency channel  $k_i$  and transmission timing offset  $T_i^{\text{d}}$  [msec] to each node by utilizing the knowledge of the UL packet generation cycle of each node. The GW transmits

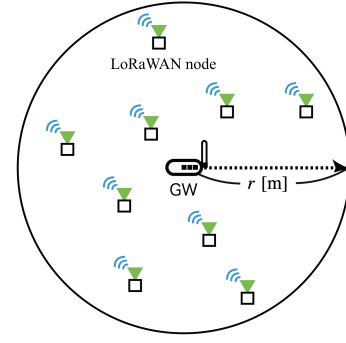


Fig. 1. Communication area.

TABLE I  
SNR AND SIR THRESHOLDS [11], [12].

SF	SNR threshold $\Gamma_S^{\text{SNR}}$ dB	SIR threshold $\Gamma_S^{\text{SIR}}$ dB
7	-7.5	-11
8	-10	-13
9	-12.5	-16
10	-15	-19

the control information to node  $i$  so that node  $i$  transmits a UL packet at the appropriate frequency channel and transmission timing for collision avoidance.

Since each node periodically transmits UL packets, the GW can estimate the UL packet generation cycle of the node once the GW successfully receives packets from a specific node multiple times. The estimated UL packet generation cycle enables the GW to estimate each node's UL packet transmission timing. Therefore, the GW can predict packet collisions by comparing the estimated transmission timing of each node. The following is the general flow of the proposed algorithm.

#### 1: UL packet generation cycle $G_{p,i}$ estimation

The GW estimates each node's UL packet generation cycle based on the reception timing of UL packets.

#### 2: Packet collision prediction

The GW checks whether packet collisions occur between the intended node and the other nodes in the subsequent packet transmission.

#### 3: Transmission timing offset candidate calculation

If the GW predicts a packet collision in the subsequent packet transmission, the GW derives transmission timing offset candidates that avoid packet collisions.

#### 4: Exploration of frequency channel and transmit offset time

From the candidate set of transmission timing offsets, the GW determines appropriate frequency channel  $k_i$  and transmission timing offset  $T_i^{\text{d}}$ .

The following subsections will explain the detail of each step of the proposed algorithm.

#### A. UL packet generation cycle estimation

Each UL packet of node  $i$  includes the frame counter (FCntUp),  $n_i$ , in the packet header [13]. Thus, the GW can know how many times the packet has been successfully received. The GW estimates the UL packet generation cycle  $G_{p,i}$  of

node  $i$  once the GW successfully receives UL packets more than once. The UL packet generation period,  $G_{p,i}$ , is very large compared to packet transmission duration  $T_{L,i}$ . Thus, the GW can easily estimate  $G_{p,i}$  from the receive timing of multiple packets and their FCntUP values, ignoring packet transmission duration  $T_{L,i}$ . Based on the above observation, the GW can estimate the following parameters of each node once it successfully receives more than one UL packet from node  $i$ : UL packet generation cycle  $G_{p,i}$ , first packet generation time  $T_i^{\text{FP}}$ , and packet transmission duration  $T_{L,i}$ .

### B. Packet collision prediction

Based on the estimated UL packet generation cycle  $G_{p,i}$  and reception time  $T_{n_i}$  of the  $n_i$ th UL packet, the GW can estimate the scheduled transmission timing of the subsequent UL packets from node  $i$ . In addition, the GW can predict the occurrence of packet collisions in advance by comparing each node's scheduled packet reception timings. Thus, after receiving the  $n_i$ th packet from node  $i$ , the GW estimates the scheduled packet transmission timings of all the nodes during the packet collision prediction period  $T_i^{\text{pred}}$  from packet reception time  $T_{n_i}$ . The packet collision prediction period,  $T_i^{\text{pred}}$ , is defined as

$$T_i^{\text{pred}} = G_{p,i} - T_{L,i} + G_p^{\text{max}}. \quad (3)$$

Let  $M_i$  denote the number of packets generated by node  $i$  within  $T_i^{\text{pred}}$ , which is given as

$$M_i = \lfloor T_i^{\text{pred}} / G_{p,i} \rfloor, \quad (4)$$

where  $\lfloor x \rfloor$  is the floor function. The definition in Eq. (3) allows for a constant time margin before the first packet and after the last packet in packet collision prediction period  $T_i^{\text{pred}}$ . After receiving a UL packet from node  $i$ , the GW judges whether the transmission period overlaps with that of other nodes in each frequency channel for each of  $M_i$  UL packets of node  $i$  in the packet collision prediction period  $T_i^{\text{pred}}$ . Let us define the overlap judgment function  $f(T_i^{\text{d}})$  for the  $(n_i + m)$ th packet at the currently allocated transmission timing offset  $T_i^{\text{d}}$  as

$$f(T_i^{\text{d}}) = \begin{cases} 0 & \text{if No overlap} \\ 1 & \text{otherwise} \end{cases}. \quad (5)$$

If Eq. (5) results in an overlap, the node is likely to have a packet collision.

### C. Transmission timing offset candidate calculation

Next, the GW calculates a transmission timing offset candidate  $T_{i,m,k}^{\text{off}}$  for the  $(n_i + m)$ th packet in frequency channel  $k$  for node  $i$  where the packet collision is predicted. Let  $\mathcal{T}'_e = \{T_1^e, \dots, T_{i'}^e, \dots, T_{I'}^e\}$  denote the set of packet transmission end timings of other nodes in the packet collision prediction period, and  $T_{n_i}^G$  denote the packet generation time of node  $i$ . The algorithm for calculating a transmission timing offset candidate  $T_{i,m,k}^{\text{off}}$  is shown in Algorithm 1. Let  $\mathcal{T}_i^{\text{off}}$  be the set of transmission timing offset candidates obtained from Algorithm 1. An example is shown in Figure 2, the GW calculates candidate offsets by comparing the packet

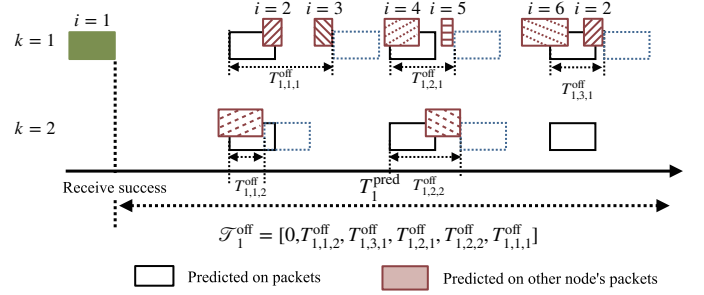


Fig. 2. Example of a transmission offset time candidate

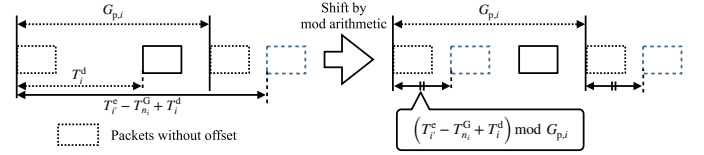


Fig. 3. Example of a transmission timing offset candidate

transmission timings of node  $i = 1$  and other nodes. If a packet collision occurrence is predicted by Eq. (5), then lines 5 through 16 are executed to calculate the transmission timing offset candidate. Here, the transmission timing offset to avoid overlapping transmission periods with other nodes is calculated by comparing the transmission completion time of other nodes with the start time of their transmission. In particular, as shown in line 9 of Algorithm 1, we calculate it using the equation given as

$$T_{\text{temp}}^{\text{off}} = (T_{i'}^e - T_{n_i}^G + T_i^{\text{d}}) \bmod G_{p,i}. \quad (6)$$

If the proposed algorithm is continued to run, the transmission timing offset  $T_i^{\text{d}}$  may become larger than the UL packet generation cycle  $G_{p,i}$ . Therefore, by adopting the mod operation in Eq. (6), the transmission timing offset  $T_i^{\text{d}}$  can be shifted to the same position in units within the UL packet generation cycle  $G_{p,i}$ , as shown in Fig. 3.

### D. Exploring Frequency Channels and Transmission Offset Time

The GW allocates frequency channel  $k_i$  and transmission timing offset  $T_i^{\text{d}}$  to node  $i$ . Thus, the GW needs to explore the appropriate transmission timing offset from the candidate set  $\mathcal{T}_i^{\text{off}}$ . In a WSN, the delay between the data generation and its reception at the GW should be as little as possible. Thus, the exploration policy of candidate set  $\mathcal{T}_i^{\text{off}}$  is to avoid packet collision while minimizing the transmission timing offset. The GW calculates predicted packet collision count  $\hat{N}_{T_{i,k}^{\text{d}}}^{\text{d}}$  for each transmission timing offset candidate. Let  $g(T_{i,k}^{\text{d}})$  denote the function to calculate predicted number of packet collisions  $\hat{N}_{T_{i,k}^{\text{d}}}$  for transmission timing offset  $T_{i,k}^{\text{d}} \in \mathcal{T}_i^{\text{off}}$ . The transmission timing offset of node  $i$ ,  $T_{i,k}^{\text{d}}$ , which minimizes  $\hat{N}_{T_{i,k}^{\text{d}}}$ , is given by

$$T_i^{\text{d}} = \operatorname{argmin}_{T_{i,k}^{\text{d}} \in \mathcal{T}_i^{\text{off}}} g(T_{i,k}^{\text{d}}) \quad (7)$$

Note that frequency channel  $k_i$  is allocated to the one corresponding to  $T_i^{\text{d}}$  determined by Eq. (7). The GW generates a

**Algorithm 1** Algorithm for calculating transmission timing offset candidate

```

1: Input:
2:  $\mathcal{I}'_e, T_{n_i}^G, T_i^d$ 
3: Initialization:
4:  $\mathcal{T}_i^{\text{off}} = \emptyset$ 
    $T_{\text{temp}}^{\text{off}} = 0$ 
5: for  $k = 1 \dots K$  do
6:   Ascending sort  $\mathcal{I}'_e = \{T_1^e, \dots, T_{i'}^e, \dots, T_{I'}^e\}$ 
7:   for  $m = 1 \dots M$  do
8:     for  $i' = 1 \dots I'$  do
9:        $T_{\text{temp}}^{\text{off}} = (T_{i'}^e - T_{n_i}^G + T_i^d) \bmod G_{p,i}$ 
10:      if  $f(T_{\text{temp}}^{\text{off}}) = 0$  then
11:         $\mathcal{T}_i^{\text{off}} = \mathcal{T}_i^{\text{off}} \cup T_{\text{temp}}^{\text{off}}$ 
12:      Break
13:    end if
14:  end for
15: end for
16: end for
17: Output:
18:  $\mathcal{T}_i^{\text{off}} = \{T_{i,1,1}^{\text{off}}, \dots, T_{i,m,k}^{\text{off}}, \dots, T_{i,M,K}^{\text{off}}\}$ 

```

TABLE II  
SIMULATION PARAMETERS.

Simulation radius, $r$	895 [m]
Simulation time, $T$	720 [min]
Number of nodes, $I$	500
Transmit power, $P_t$	13 [dBm]
Carrier frequency, $f_c$	0.923 [GHz]
Bandwidth, $W$	125 [kHz]
Number of frequency channels, $K$	{1, 2, 4}
SF, $S$	{7, 8, 9, 10}
Coding rate, $R$	4/7
Duty cycle, $D_c$	0.01
Noise power spectrum density, $N_0$	-174 [dBm/Hz]
Noise figure, $NF$	10 [dB]
Path loss coefficient, $\alpha$	4.0
Propagation offset, $\beta$	9.5
Frequency loss component, $\eta$	4.5
Overhead symbol, $O_{\text{sym}}$	20.25
Packet data size, $B_{\text{data}}$	160 [bits]
Maximum UL packet generation cycle, $G_p^{\text{max}}$	10 [min]
CS threshold, $\Gamma^{\text{CS}}$	-110 [dB]
Minimum backoff exponent, $n_{\text{min}}^{\text{CS}}$	7
Maximum number of CS repetitions, $N_{\text{max}}^{\text{CS}}$	13
Fixed length slot time, $T_{\text{slot}}^{\text{CS}}$	1.024 [msec]

DL packet containing the allocation control information for the new frequency channel  $k_i$  and the transmission timing offset  $T_i^d$ , and transmits it to node  $i$ .

## IV. SIMULATION AND RESULTS

### A. Simulation Parameters

The LoRaWAN system parameters are listed in Tables II, which follow the Japanese parameter configuration AS923 [13].  $I = 500$  nodes are placed randomly and uniformly in a communication area of  $r = 895$  [m] radius, where  $r = 895$  [m] is the maximum possible communication distance at SF of 10 under the channel model considered. Each node randomly selects its UL packet cycle from 1 ~ 10 [min].

### B. Channel Model

Without loss of generality, the channel model only considers path loss because this paper tries to evaluate the impact of traffic control on communication quality.

The received signal power of node  $i$  at the GW is given by

$$P_{r,i} = P_t - P_{\text{Loss}}(d_i), \quad (8)$$

where  $P_t$  [dBm] is the transmit power common to the nodes and GW, and  $P_{\text{Loss}}(d_i)$  [dB] is the path loss component with  $d_i$  [m] being the physical distance between node  $i$  and the GW. The path loss component,  $P_{\text{Loss}}(d_i)$  [dB], is given as [14]

$$P_{\text{Loss}}(d_i) = 10\alpha \log_{10} d_i + \beta + 10\eta \log_{10} f_c, \quad (9)$$

where  $\alpha, \beta$ , and  $\eta$  are the path loss coefficient, offset, and frequency loss component, respectively,  $f_c$  [GHz] is the carrier frequency. Since there is a reciprocity between the UL and DL channels, the received signal power of the GW at node  $i$  is assumed to be equal to  $P_{r,i}$ , which is given in (8).

### C. Comparison Method

For performance comparison, this paper considers ALOHA and LBT. In ALOHA, each node transmits a UL packet upon its generation. Node  $i$  randomly selects frequency channel  $k_i \in \mathcal{K}$  for each UL packet transmission, i.e., frequency hopping is applied.

As an LBT, we adopt a CS-based version that is less complex than CSMA/CA. In LBT, node  $i$  performs CS for  $T^{\text{CS}}$  [sec] at frequency channel  $k_i$  once it generates a UL packet. Let the CS threshold be  $\Gamma^{\text{CS}}$  [dBm]. If the node does not detect any other node's signal during  $T^{\text{CS}}$ , the node transmits its UL packet immediately once the CS ends. On the other hand, if the node detects the signal of another node, it waits for transmission using binary backoff after the CS ends. After waiting for the backoff time, the node carries out CS. The node repeats CS until its carry-out reaches the maximum number of CS repetitions  $N_{\text{max}}^{\text{CS}}$  for a one UL packet. The backoff time  $T_{\text{back}}^{\text{CS}}$  [msec] is given by

$$T_{\text{back}}^{\text{CS}} = \mathcal{U}\left(0, 2^{n_{\text{min}}^{\text{CS}} + n_r^{\text{CS}}}\right) \times T_{\text{slot}}^{\text{CS}}, \quad (10)$$

where  $n_{\text{min}}^{\text{CS}}$  is the minimum backoff exponent,  $n_r^{\text{CS}}$  is the number of iterations of waiting by CS in one packet transmission, and  $T_{\text{slot}}^{\text{CS}}$  is the fixed length slot time. Note that  $n_{\text{min}}^{\text{CS}} + n_r^{\text{CS}} \leq N_{\text{max}}^{\text{CS}}$  is satisfied.

### D. Performance Metrics

1) *Packet Delivery Rate*: We define a *cycle* as the maximum UL packet generation cycle, which is indexed by  $c \in \{1, \dots, c, \dots, C\}$ . For example,  $c = 1$  represents the period from the system start time to the maximum UL packet generation cycle. The PDR during the  $c$ th observation period is defined as

$$\text{PDR}_c \triangleq \frac{\sum_{i=1}^I N_{i,c}^{\text{succ}}}{\sum_{i=1}^I N_{i,c}^{\text{tran}}}, \quad (11)$$

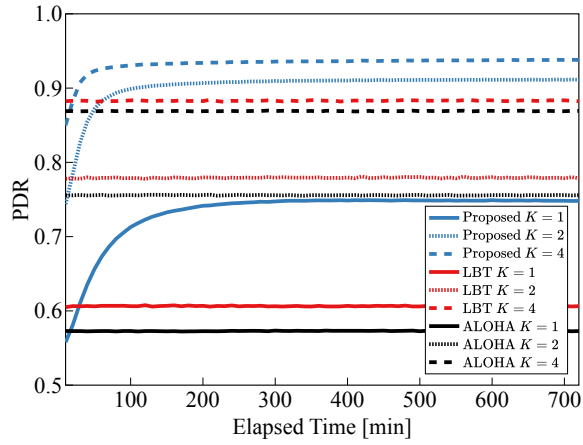


Fig. 4. Average PDR of the comparison method and proposed scheme

where  $N_c^{\text{succ}}$  is the number of UL packets of node  $i$  successfully received by the GW and  $N_c^{\text{tran}}$  is the total number of packets transmitted by node  $i$  during the  $c$ th cycle, respectively.

The PDR of each node is also evaluated. The PDR of node  $i$  from the start to the end of the system is defined as

$$\text{PDR}_i \triangleq \frac{\sum_{c=1}^C N_{i,c}^{\text{succ}}}{\sum_{c=1}^C N_{i,c}^{\text{tran}}}, \quad (12)$$

2) *Age of information*: The AoI is defined as the difference between the timestamp of the latest data obtained by the information aggregation station and the current time. So, in order to evaluate the AoI of each node in this paper, the node  $i$ 's AoI  $A_{i,t}$  [sec] at time  $t$  is defined as

$$A_{i,t} \triangleq t - g_{t,i}, \quad (13)$$

where  $g_{t,i}$  is the latest packet generation time of node  $i$  that the GW has successfully received until time  $t$ . Note that  $g_{t,i}$  does not change unless a new packet from node  $i$  is successfully received, so  $A_{i,t}$  increases monotonically.

Next, we define the time average of the AoI for node  $i$ . Let  $J_i$  be the number of UL packets of node  $i$  successfully received by the GW, then average AoI  $\bar{A}_i$  [sec] is given by

$$\bar{a}_i \triangleq \frac{1}{T} \sum_{j=0}^{J_i} \left( \frac{G_{p,i}^2}{2} + G_{p,i} D_{i,j} \right), \quad (14)$$

where  $D_{i,j}$  [sec] is the delay time between the generation of the  $j$ th packet and its receiving by the GW.  $D_{i,j}$  is given as

$$D_{i,j} = r_{i,j} - g_{i,j}, \quad (15)$$

where  $r_{i,j}$  is the received time of the  $j$ th packet at the GW, and  $g_{i,j}$  is the generated time of the  $j$ th packet at node  $i$ .

To take into account the worst-case value of the AoI, we also define the AoI just before this jump as the peak AoI (PAoI) [15], which is given as

$$A_{i,j}^{\text{peak}} \triangleq r_{i,j} - g_{i,j-1} \quad (16)$$

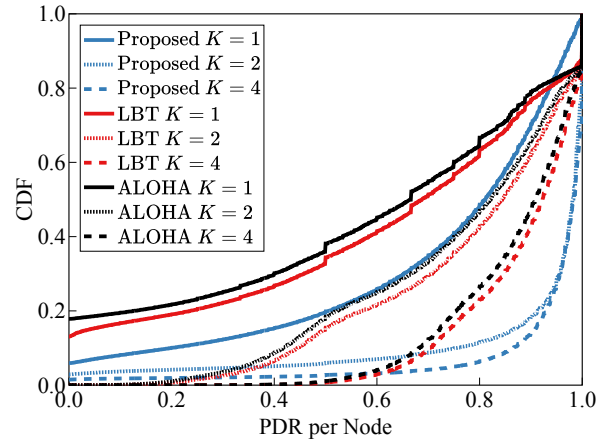


Fig. 5. CDF of the PDR for each node.

## E. Numerical Results

1) *PDR*: Fig. 4 shows the average PDR performance as a function of elapsed time. From Fig. 4, the average PDR performance of the proposed scheme improves with time, irrespective of the number of frequency channels. This is because the GW transmits control signals to more nodes as time elapses; hence, the number of nodes using the communication resource where packet collisions occur decreases. Especially when the number of frequency channels is  $K = 1$ , the proposed scheme can improve the average PDR performance by up to about 18% compared with ALOHA. In addition, the proposed scheme has better average PDR performance than ALOHA and LBT, irrespective of the number of frequency channels. The PDRs of the proposed scheme tend to converge faster when the number of channels is larger. This is because it is easier to explore wireless resources to avoid continuous packet collisions due to the sufficient amount of radio resources when the number of channels is large. The LBT has a slightly better average PDR performance than the ALOHA due to CS. However, LBT has lower PDR performance than the proposed scheme because CS does not work well due to the long distance between nodes caused by the large communication area. When the number of frequency channels is  $K = 1$ , the proposed scheme can improve the average PDR performance by up to about 16% compared with LBT. Fig. 5 shows the cumulative distribution function (CDF) performance of the PDR for each node. As shown in Fig. 5, the proposed scheme has superior CDF performance compared to ALOHA and LBT in a wide range regardless of the number of frequency channels. However, in a high PDR region with  $K = 1$ , the proposed scheme degrades the CDF performance compared to ALOHA and LBT. This degradation is because the proposed algorithm changes the transmission timing of each node to avoid packet collisions, which may cause packet collisions between nodes in combinations that do not occur in ALOHA and LBT. Also, when the number of frequency channels is  $K = 2, 4$ , and the PDR is low, the performance of the proposed scheme is degraded compared to ALOHA and LBT. This degradation is because the proposed scheme does not apply frequency hopping; thus, there are some nodes the GW cannot control

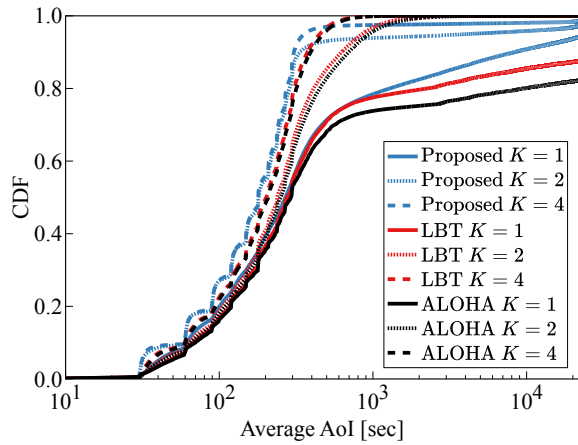


Fig. 6. CDF of average AoI.

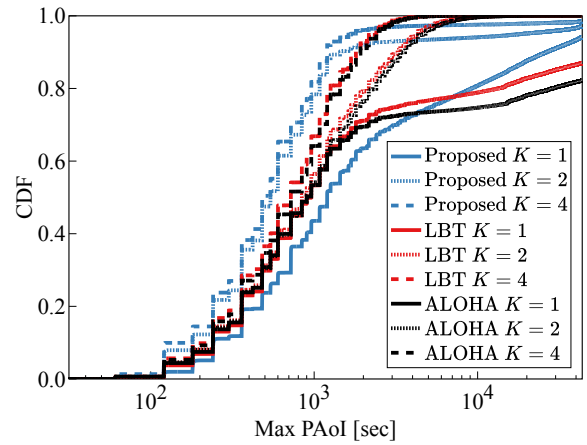


Fig. 7. CDF of max PAoI.

due to constantly happening packet collisions.

2) *AoI*: Fig. 6 shows the CDF performance of the average AoI for each node. From Fig. 6, the proposed scheme provides better CDF performance in the low AoI region compared to ALOHA and LBT irrespective of the number of frequency channels. This is because the effects of successfully transmitting packets continuously through packet collision avoidance are greater than the effects of the delay caused by some offset time allocation by the proposed scheme. In addition, when the number of frequency channels is large, the proposed scheme can effectively avoid packet collision by appropriately selecting a frequency channel for each node. As a result, the offset value required for packet collision avoidance is reduced. Therefore, the proposed scheme tends to improve the CDF performance of the average AoI against ALOHA and LBT more when the number of frequency channels is more.

Fig. 7 shows the CDF performance of the max PAoI for each node. From Fig. 7, the proposed scheme has better CDF performance in the low PAoI region compared to ALOHA and LBT when the number of frequency channels is  $K = 2, 4$ . This is because the proposed scheme avoids packet collisions with small offset values. Note that the PAoI represents the worst-case value of the AoI and thus is highly sensitive to continuous packet collisions. On the other hand, when the number of frequency channels is  $K = 1$ , the offset value tends to be large, so the proposed scheme has a degraded CDF performance of PAoI compared to ALOHA and LBT.

## V. CONCLUSION

This paper proposed a centralized radio resource allocation scheme that aims to avoid packet collisions in periodic traffic in LPWANs, taking into account the characteristics of the periodical traffic. A GW predicts packet collisions and allocates for nodes frequency channels and transmission timing offset that can avoid the predicted packet collisions. Computer simulations have shown that the proposed scheme can improve the average PDR performance by up to about 18% and 16% compared to ALOHA and LBT, respectively.

## ACKNOWLEDGMENT

This research and development work was supported by the MIC/SCOPE JP205004001.

## REFERENCES

- [1] A. Zanella, N. Bui, A. Castellani, L. Vangelista, and M. Zorzi, "Internet of Things for Smart Cities," *IEEE Internet Things J.*, vol. 1, no. 1, pp. 22–32, 2014.
- [2] O. Georgiou and U. Raza, "Low Power Wide Area Network Analysis: Can LoRa Scale?" *IEEE Commun. Lett.*, vol. 6, no. 2, pp. 162–165, 2017.
- [3] J. Ortín, M. Cesana, and A. Redondi, "Augmenting LoRaWAN Performance With Listen Before Talk," *IEEE Trans. Wireless Commun.*, vol. 18, no. 6, pp. 3113–3128, Jun. 2019.
- [4] L. Beltramelli, A. Mahmood, P. Österberg, and M. Gidlund, "LoRa Beyond ALOHA: An Investigation of Alternative Random Access Protocols," *IEEE Trans. Ind. Informat.*, vol. 17, no. 5, pp. 3544–3554, 2021.
- [5] A. H. Nguyen, Y. Tanigawa, and H. Tode, "Scheduling Method for Solving Successive Contentions of Heterogeneous Periodic Flows Based on Mathematical Formulation in Multi-Hop WSNs," *IEEE Sens. J.*, vol. 18, no. 21, pp. 9021–9033, 2018.
- [6] S. Kaul, M. Gruteser, V. Rai, and J. Kenney, "Minimizing Age of Information in Vehicular Networks," in *Proc. 2011 8th Annu. IEEE Commun. Soc. Conf. on Sensor, Mesh and Ad Hoc Commun. and Netw.*, pp. 350–358, 2011.
- [7] S. Kaul, R. Yates, and M. Gruteser, "Real-Time Status: How Often Should One Update?" in *Proc. 2012 IEEE INFOCOM*, pp. 2731–2735, 2012.
- [8] M. Moltafet, M. Leinonen, and M. Codreanu, "Worst Case Age of Information in Wireless Sensor Networks: A Multi-Access Channel," *IEEE Wireless Commun. Lett.*, vol. 9, no. 3, pp. 321–325, 2020.
- [9] R. K. Verma, S. Bharti, and K. K. Pattanaik, "GDA: Gravitational Data Aggregation Mechanism for Periodic Wireless Sensor Networks," in *Proc. 2018 IEEE SENSORS*, pp. 1–4, 2018.
- [10] V. Gupta, S. K. Devar, N. H. Kumar, and K. P. Bagadi, "Modelling of IoT Traffic and Its Impact on LoRaWAN," in *Proc. IEEE GLOBECOM*, pp. 1–6, Dec. 2017.
- [11] Semtech, "Semtech SX1272 Datasheets," [online]. Available: <https://www.semtech.com/products/wireless-rf/lora-core/sx1272>.
- [12] D. Croce, M. Gucciardo, S. Mangione, G. Santaromita, and I. Tinnirello, "Impact of LoRa Imperfect Orthogonality: Analysis of Link-Level Performance," *IEEE Commun. Lett.*, vol. 22, no. 4, pp. 796–799, Apr. 2018.
- [13] LoRa Alliance, "LoRaWAN Regional Parameters v1.1rB," [online]. Available: [https://lora-alliance.org/sites/default/files/2018-04/lorawantm\\_regional\\_parameters\\_v1.1rb\\_-\\_final.pdf](https://lora-alliance.org/sites/default/files/2018-04/lorawantm_regional_parameters_v1.1rb_-_final.pdf), Dec. 2018.
- [14] P. Series, "Propagation Data and Prediction Methods for the Planning of Short-Range Outdoor Radiocommunication Systems and Radio Local Area Networks in the Frequency Range 300 MHz to 100 GHz," [online]. Available: <https://www.itu.int/rec/R-REC-P.1411-9-201706-S/en>, 2017.
- [15] M. Costa, M. Codreanu, and A. Ephremides, "On the Age of Information in Status Update Systems With Packet Management," *IEEE Trans. Inf. Theory*, vol. 62, no. 4, pp. 1897–1910, 2016.